

The *Arabidopsis* checkpoint protein Bub3.1 is essential for gametophyte development

Inna Lermontova, Joerg Fuchs, Ingo Schubert

Leibniz-Institute of Plant Genetics and Crop Plant Research (IPK), D-06466 Gatersleben, Germany

TABLE OF CONTENTS

1. Abstract
2. Introduction
3. Materials and methods
 - 3.1. Plant material
 - 3.2. Gene cloning and RT-PCR analysis
 - 3.3. Generation of Bub3.1-ECFP and EYFP-Bub3.1 fusion constructs
 - 3.4. Analysis of T-DNA insertion mutants
 - 3.5. Whole-mount preparation
 - 3.6. Alexander staining
 - 3.7. Western blot analysis
4. Results
 - 4.1. Cloning and sequence comparison of *Arabidopsis* Bub3 homologues
 - 4.2. Expression of *Arabidopsis* Bub3 in different organs
 - 4.3. Subcellular localization of Bub3.1-ECFP and EYFP-Bub3.1 fusion proteins
 - 4.4. Identification and characterization of T-DNA insertion mutants for Bub3 genes
 - 4.5 Characterization of an embryo lethal bub3.1 mutant (GABI-362D05)
5. Discussion
6. Acknowledgement
7. References

1. ABSTRACT

Except for Mad2 homologues of maize and wheat, no spindle checkpoint proteins which regulate the onset of anaphase during nuclear divisions have been reported for plants so far. We found three homologues of the spindle checkpoint protein Bub3 in *Arabidopsis thaliana*. Bub3.1 and Bub3.2 are 88% identical at the amino acid level, while Bub3.3 is more distantly related. Bub3.1 and Bub3.2 mRNA appeared preferentially in mitotically active tissues. Bub3.1 but not Bub3.2 showed increased expression during mitosis. Nuclear but no centromeric localization was shown for EYFP-Bub3.1 and Bub3.1-ECFP fusion constructs. Three T-DNA insertion mutants each were identified for Bub3.1 and Bub3.2 encoding genes. One *bub3.1* mutant survived only in heterozygous state and displayed defects in development of male and female gametophytes, while two other homozygous *bub3.1* mutants revealed transcripts and are therefore no null mutants. In contrast, all three homozygous *bub3.2* mutants appeared to be viable and fertile without generating full-length transcripts.

2. INTRODUCTION

Checkpoint kinetochore proteins (KPs) control the entry into mitosis and meiosis (1). Spindle checkpoint genes, first identified in budding yeast, include the 'mitotic arrest defective' genes *Mad1-3* (2) and the 'budding uninhibited by benzimidazole' genes *Bub1* and *Bub3* (3) and are highly conserved among eukaryotes. The spindle checkpoint control proteins were intensively studied in yeast, *Drosophila*, *C. elegans* and mammals (for review see (4, 5). In plants, only maize and wheat homologues of yeast Mad2 were identified and localized at kinetochores from prometaphase until the onset of anaphase (6, 7). Like other cell cycle checkpoints, the spindle checkpoint consists of sensors, signal transducers and a target. The sensors (presumably the motor protein CENP-E, AuroraB/Ipl1, Rod/Zw10) and their monitoring of incomplete or defective metaphase congression and spindle fiber attachment to centromeres remain to be elucidated in detail. The signal transduction involves Mad1-3; Bub1, 3 and Mps1 proteins, which localize transiently to kinetochores (8-10). Without bipolar attachment of sister kinetochores to spindle

microtubules, tension at kinetochores is lacking and the spindle checkpoint is active. A single unattached kinetochore can prevent anaphase onset (11) by blocking the activation of the target, the anaphase-promoting complex/cyclosome (APC/C), via preventing the integration of Cdc20 into this complex (12). In yeast, *Xenopus*, and mammalian cells, Cdc20 is bound either i) by Mad2, which is recruited to kinetochores by Mad1, ii) by the BubR1 (= Mad3 in yeast) -Bub3 complex, or iii) by the mitotic checkpoint complex (MCC) consisting of Mad2, BubR1 -Bub3 (13-15). When tension arises due to bipolar spindle fiber attachment at sister-kinetochores, signal transduction mediates release of checkpoint proteins from kinetochores, dissociation of their complex (es) with Cdc20, formation of an APC-Cdc20 complex and eventually transition to anaphase. APC-Cdc20 mediates ubiquitination and degradation of securin. This leads to activation of separase, which cleaves those cohesins that hold sister chromatids at centromeres together. Subsequently, sister chromatids may separate and move along spindle fibers to opposite poles (for review see (5)).

Although the checkpoint KPs are highly conserved, their role may differ between organisms as demonstrated by approaches to inactivate KP genes. In *S. cerevisiae*, *bub* and *mad* mutants are viable, though the growth of mutant cells is slowed down (16). In *S. pombe*, *bub1* null mutants are viable but show abnormalities in mitotic chromosome segregation (17). In *Drosophila*, loss of *bub1* is lethal at the larval/pupal transition (18).

To characterize spindle checkpoint proteins in plants, *Arabidopsis* homologues encoding the spindle checkpoint protein Bub3 were cloned. Tissue-specific expression of endogenous Bub3 and intracellular localization of recombinant fluorescent Bub proteins as well as the viability of homozygous *versus* heterozygous T-DNA insertion mutants were studied.

3. MATERIALS AND METHODS

3.1. Plant material

Plants of *Arabidopsis thaliana* ecotype Columbia were cultivated in growth chambers in a 16-h-light/8-h-dark cycle at 20°C. For expression studies, tissue samples were harvested from 2- to 4-week-old plants. T-DNA tagged lines for At3g19590 (*Bub3.1*) and At1g49910 (*Bub3.2*) were obtained from SAIL (Syngenta Arabidopsis Insertion Library) (19), GABI-Kat (20) and SALK (The Salk Institute Genomic Analysis Laboratory) T-DNA mutant collections.

3.2. Gene cloning and RT-PCR analysis

To amplify full-length cDNAs for Bub3, oligonucleotide primers corresponding to *AtBub3.1* (forward, 5'-ATA CTC GAG ATG ACG ACT GTG ACT CCG TC -3'; reverse, 5'-AAT GGT ACC CGC CGC AGG ATT CGG GTA TAC-3') and *AtBub3.2* (forward, 5'-TAA CTC GAG ATG ACT TTG GTG CCG GCC ATT G-3'; reverse, 5'-TTA GGT ACC TAC CGG GGG ATT TGG GTA TAC-3') were used for RT-PCR (RevertAid HMinus

First Strand cDNA Synthesis kit; Fermentas). At the 5'-end of the primers, a restriction site for *XhoI* or *KpnI* was added. mRNA of seedlings, flower buds, roots, leaves, and stems was isolated using poly-U-coated magnetic beads (Dyanal). The RT-PCR products were cloned into the pCR 2.1-TOPO vector (Invitrogen). For semi-quantitative RT-PCR of *Bub3* and EF-1 alpha as a control gene, the following primers were used: *Bub3.1* (P1-5'-CTT CAA CGG GAA AAA TGA CGA CTG TGA CTC-3'; P2-5'-AAC TTG TGT TTC TTC CTT TCT ACG CCG CAG-3'; P3-5'-CCT AAT GGA ATA TGC TCT TAG CTC TGT TG-3'; P4-5'-CAA CAG AGC TAA GAG CAT ATT CCA TTA GG-3'), *Bub3.2* (P1-5'-ATT CGT ATT TTC CAG GAT GAC TTT GGT GCC-3'; P2-5'-TGA CTC TGC TCA TTC CAT TAT TTC TTG AC-3'; P3-5'-CCA ACG GAA CAG GAT ATG CCC TTA GCT CTG-3'; P4-5'-CAG AGC TAA GGG CAT ATC CTG TTC CGT TGG-3'), *EF - 1 alpha - a4* (At1g07940) (forward, 5'-GCT GTT CTT ATC ATT GAC TCC ACC ACT-3'; reverse, 5'-GGC ACC GTT CCA ATA CCA CCA AT-3'). To avoid contamination with genomic DNA, total RNA used for semi-quantitative RT-PCR analysis was treated with DNase. Moreover, P3 and P4 primers for both *Bub3.1* and *Bub3.2* genes were designed to cover the exon-exon junction.

3.3. Generation of Bub3.1-ECFP and EYFP-Bub3.1 fusion constructs

To generate a p35S:Bub3.1-ECFP fusion construct, the *Bub3.1* sequence was cut out from the pCR2.1-TOPO vector using *XhoI* and *KpnI*, and inserted in frame with ECFP into the pWEN15 vector digested with the same restriction enzymes. The resulting expression cassette including 35S promoter, Bub3.1-ECFP and Nos terminator was digested by *HindIII* and *PacI* (blunt end) and subcloned into the pGPTV-Bar plant transformation vector digested with *HindIII* and *EcoRI* (blunt end). For the generation of a p35S:EYFP-Bub3.1 fusion construct, the *Bub3.1* sequence was amplified with the primer pair 5'-TAG AAT TCA TGA CGA CTG TGA CTC CGT CCG-3' and 5'-TAG TCG ACC TAC GCC GCA GGA TTC GGG TAT-3' from the pCR2.1-TOPO vector, generating a *EcoRI* linker sequence at the 5' end and *SalI* linker sequence at the 3' end. The amplified fragment was inserted into the p35S-BAM-EYFP vector (21) in frame with EYFP. The resulting expression cassette including 35S promoter, EYFP-Bub3.1 and Nos terminator was subcloned into the pLH7000 vector (<http://www.dna-cloning-service.de>) via the *SfiI* restriction site.

3.4. Analysis of T-DNA insertion mutants

Segregation of the sulfadiazine and phosphinotricine (PPT) resistance markers encoded by GABI and SAIL T-DNA tags, respectively, was assayed by growing seedlings in MS medium containing 5 mg/l sulfadiazine or 16 mg/l PPT. To confirm the presence and to identify heterozygous *versus* homozygous state of T-DNA insertion, we performed PCR with pairs of gene-specific primers flanking the putative positions of T-DNA in Bub3.1: GABI-068-A03-LP (5'-ATC TTC AAC GGG AAA AAT GAC GAC T-3') and GABI-068-A03-RP (5'-AAT CAA CAA CTT CTG AGC AGC CAA T -3');

GABI-362-D05-LP (5'- AAG AAG GGA GTC TTC ACT GAA ATA CCA-3') and GABI-362-D05-RP (5'- GAA ATC TAT GAA ACA GTT GGG CTC CT-3'); SALK-031919-LP (5'- TTG GAG CTG ATT GAT CCA AAG-3') and SALK-031919-RP (5'- TCA GTC GAG ATG GTC AGC TG-3'); in Bub3.2: SALK-151687-LP (5'- TGA ATG GAA ACA ATC AGG TTT C-3') and SALK-151687-RP (5'- TGT TTA GGA ATT GTT TTG CGG-3'); SAIL-1288-E06-LP (5'- ATG TTT ATG TGG CGT TAT AGG GCA AGT G-3') and SAIL-1288-E06-RP (5'- CGC CGT AGA CTA CCA CAG TTC ATC AAA G-3'); SAIL-675-D09-LP (5'- CTT TGA GGG CTA ATT CAG AGT ATT GGG ATT-3') and SAIL-675-D09-RP (5'- TCT GTA AGT CTC AAT GGT CAA TGT CCA CAA-3'); and with a pair of gene-specific and the following corresponding T-DNA end-specific primers: LB-GABI (5'- CCC ATT TGG ACG TGA ATG TAG ACA C-3'); LB3-Syngenta (5'- TAG CAT CTG AAT TTC ATA ACC AAT CTC GAT ACA C-3') and LB-SALK (5'- GCG TGG ACC GCT TGC TGC AAC T-3'), respectively.

3.5. Whole-mount preparation

Flowers and siliques of different developmental stages were fixed in ethanol-acetic acid (9:1) overnight at 4°C and dehydrated by two subsequent 1 h steps in 70% and 90% ethanol. The preparation was then cleared in chloral hydrate (chloral hydrate:water:glycerol (8:2:1)) overnight at 4°C. Pistils were dissected and observed using differential interference contrast (DIC) optics (Zeiss). Seeds in siliques were counted under a binocular (Zeiss).

3.6. Alexander staining

Flowers and flower buds were collected in 10% ethanol and incubated overnight at 10°C. Anthers were isolated and put on slides. Dissected anthers were incubated with Alexander stain (22) under coverslips for 15 min at room temperature and evaluated using a light microscope (Axiophot, Zeiss).

3.7. Western blot analysis and immunostaining

Protein extraction and Western blot analysis were performed as described (21). Plant material (100 mg) was ground under liquid nitrogen and suspended in 500 µL solubilization buffer (56mM Na₂CO₃, 56mM dithiothreitol, 2% SDS, 12% sucrose and 2 mM EDTA). After 15 min of incubation at 70°C, cell debris was removed by centrifugation. The protein concentration was determined according to Bradford (23). Protein samples were separated by SDS-PAGE in 12.5% polyacrylamide gels according to Laemmli (24). Membranes were incubated for 12 h at 10°C in TBS and 3% low-fat milk containing anti-GFP (1:500, BD Biosciences) antibodies. Secondary anti-rabbit (Bio-Rad) antibodies conjugated to horseradish peroxidase were used to visualize immunocomplexes by an enhanced chemiluminescence detection kit (Bio-Rad) according to manufacturer's instructions. Immunostaining was performed as described (21). EYFP-Bub3.1 and Bub3.1-ECFP were detected with rabbit polyclonal antisera against GFP (1:500) and goat anti-rabbit rhodamine (1:100; Jackson Immuno Research Laboratories).

4. RESULTS

4.1. Cloning and sequence comparison of *Arabidopsis* Bub3 homologues

A search in *Arabidopsis* databases for homologues of the spindle checkpoint protein Bub3 resulted in three candidate genes (At3g19590-*AtBub3.1*, At1g49910-*AtBub3.2* and At1g69400-*AtBub3.3*) encoding 340, 339 and 315 amino acids, respectively. Two proteins, Bub3.1 and Bub3.2, share 88% of their amino acid residues while *AtBub3.3* is only 37% identical to both *AtBub3.1* and *AtBub3.2*. Figure 1 shows an alignment of Bub3.1 and Bub3.2 of *Arabidopsis* and rice together with Bub3 of human, *Xenopus*, *Drosophila* and *S. pombe*. Most amino acids of Bub3 are highly conserved across species. Moreover, *Arabidopsis* Bub3 proteins contain typical WD-40 repeats, which are apparently important for multi-protein complex assembly (25). The cDNAs corresponding to *Bub3.1* and *Bub3.2* were isolated by RT-PCR. The exon/intron structure of these two *Arabidopsis* Bub3 genes was investigated applying gene prediction programs and published EST sequences, and was confirmed by comparison of cDNA and genomic sequences. To investigate the evolutionary relationship of the Bub3 family, a phylogenetic tree was constructed for the Bub3 protein sequences (Figure 2). *AtBub3.1* and *AtBub3.2* are closest related to the corresponding rice proteins, while *AtBub3.3* was more distantly related to *AtBub3.1* and *AtBub3.2* than to Bub3 of non-plant organisms. Therefore, we focused on further characterization of Bub3.1 and Bub3.2.

4.2. Expression of *Arabidopsis* Bub3 in different organs

The Bub3 expression in various organs of *Arabidopsis* was determined by semiquantitative RT-PCR on total RNA isolated from flower buds, flowers, roots, siliques, leaves and stems (Figure 3A). High abundance of Bub3 transcripts was detected in roots, flower buds, flowers and young siliques. The elongation factor was used as loading standard. Because Bub3 RNA was most abundant in extracts from tissues rich in dividing cells, we plotted the RNA profiles of the *AtBub3* genes against cell cycle progression of synchronized *Arabidopsis* tissue culture cells using publicly available Affymetrix microarray datasets (26). The *Bub3.1* gene is activated immediately after release of amphidicolin block (Figure 3B). The Bub3.1 mRNA increase coincides with the entry into mitosis, when also expression of B-type cyclin is upregulated (27, 28), and decreased towards the end of mitosis. In contrast to that, the expression of *Bub3.2* showed no obvious correlation with the mitotic cell cycle.

4.3. Subcellular localization of Bub3.1-ECFP and EYFP-Bub3.1 fusion proteins

To study the localization of Bub3, Bub3.1 was fused with ECFP on its C-terminus and with EYFP on its N-terminus and expressed under control of the CaMV 35S promoter. RT-PCR analysis performed on 10 days old F2 seedlings of transformants revealed the presence of *Bub3.1-ECFP* and of *EYFP-Bub3.1* transcripts, respectively. Western blot analysis using anti-GFP antibodies revealed the presence of fusion proteins of expected size and a

Figure 1. Sequence analysis of Bub3 proteins (A) Clustal alignment of Bub3 proteins from *Homo sapiens*, *Xenopus laevis*, *Drosophila melanogaster*, *Arabidopsis thaliana*, *Oryza sativa* and *Schizosaccharomyces pombe*. The positions of amino acid residues identical in all sequences are indicated by asterisks, one or two dots indicate positions of increasingly conserved residues. The WD40 repeats of AtBub3.1 and AtBub3.2 are shown in bold. (B) Schematic view of Bub3.1, Bub3.2 and Bub3.3 proteins of *Arabidopsis*. WD repeats are indicated.



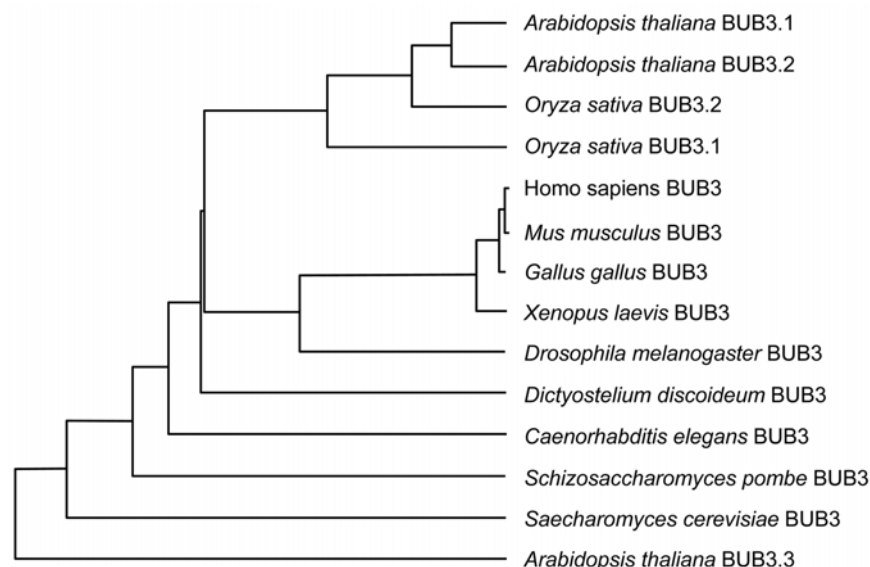


Figure 2. The phylogenetic tree of Bub3 proteins constructed by means of the TreeTop program (www.genebee.msu.su/genebee.html) with clustal algorithm.

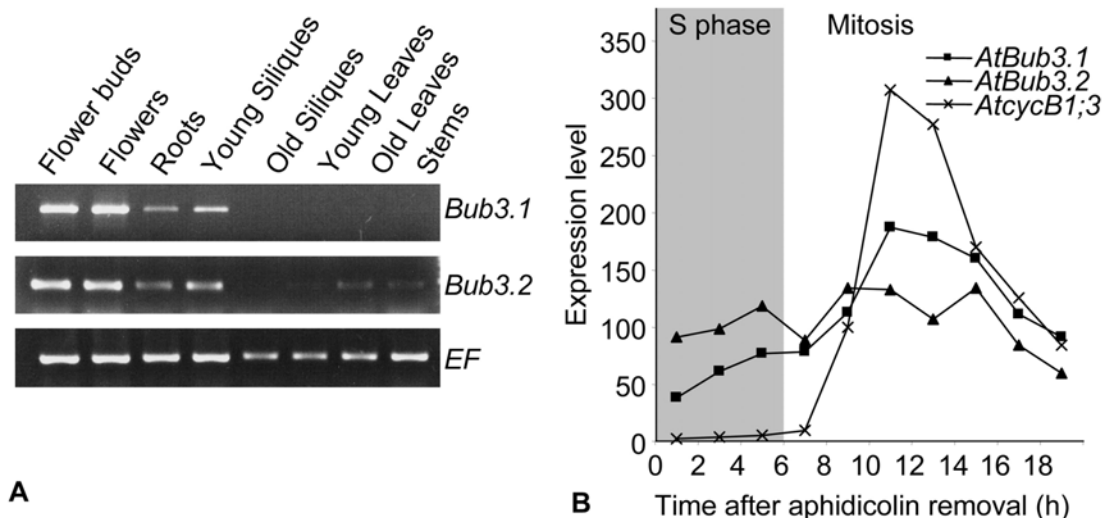


Figure 3. Transcription analysis of *AtBub3.1* and *AtBub3.2* genes. (A) *AtBub3.1* and *AtBub3.2* mRNA abundance assessed by semiquantitative RT-PCR in *Arabidopsis* flower buds, flowers, roots, young and old siliques, young and old leaves and stems. Amplification products of the elongation factor (EF) mRNA were used as a loading control. (B) mRNA profiles of *AtBub3.1*, *AtBub3.2* and *AtcycB1;3* during the mitotic cell cycle deduced from publicly available microarray data of synchronized *Arabidopsis* tissue culture cells (26).

strong variation in expression level between transformants (Figure 4). Presence and distribution of fluorescent signals were analyzed in root meristems of transgenic seedlings grown in coverslip chambers. Fluorescent signals were detected in nuclei of all transformants independent of the expression level of the fusion protein (Figure 4C). Immunostaining with anti-GFP antibodies on squashed root tip nuclei of transformants showed a uniform distribution of EYFP-Bub3.1 and Bub3.1-ECFP foci within nucleoplasm. Contrary to the expectation no clear immunofluorescence was detectable at centromere positions on prometaphase chromosomes.

4.4. Identification and characterization of T-DNA insertion mutants for *Bub3* genes

To examine the role of Bub3 in *Arabidopsis*, we tested *Arabidopsis* lines with disrupted *Bub3* genes from the Syngenta, GABI and SALK collections of T-DNA insertion mutants. For *Bub3.1*, insertions were annotated within the first intron (GABI-068-A03), the 5th intron (GABI-362-D05) and the 3'-non-coding region (SALK-031919), while in case of *Bub3.2*, two insertions were

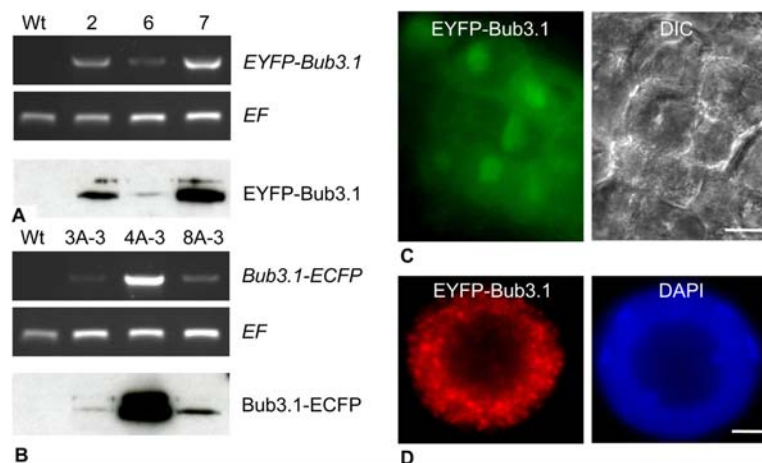


Figure 4. Expression and localization of EYFP-Bub3.1 and Bub3.1-ECFP fusion proteins in *Arabidopsis*. (A, B) Semiquantitative RT-PCR analysis of *EYFP-Bub3.1* and *Bub3.1-ECFP* mRNA (upper panels) in selected lines of corresponding transformants. Amplification products of elongation factor (EF) mRNA were used as a loading control (middle panels). Western blots of the same transgenic lines with anti-GFP antibodies are shown in the lower panels. Wt = wild type. (C) *In vivo* localization of the EYFP-Bub3.1 fusion protein in a root tip of a transformant (left), DIC image of the same root tip region (right). (D) Anti-GFP immuno-fluorescence in a nucleus of a EYFP-Bub3.1 transformant (left) and the same nucleus stained with DAPI (right). Bars: (C) 20 μ m; (D) 2 μ m.

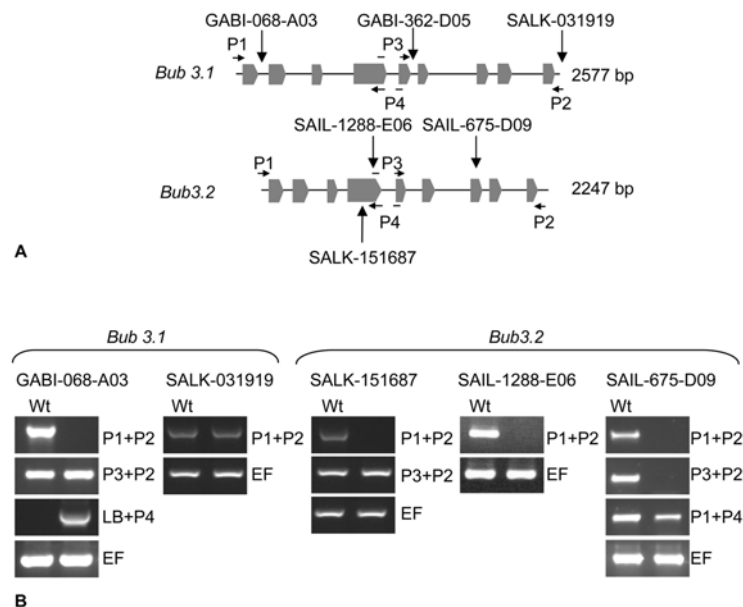


Figure 5. Insert position and expression of *bub3.1* and *bub3.2* T-DNA insertion mutants. (A) Schematic representation of the *bub3.1* and *bub3.2* alleles with the corresponding T-DNA insertions (vertical arrows). The gray boxes represent exons. The positions of primers used for RT-PCR are marked by horizontal arrows. Primers P3 and P4 designed from exon-exon junction are shown by interrupted arrows. (B) Semiquantitative RT-PCR analysis (30 cycles) of *Bub3.1* and *Bub3.2* expression in homozygous T-DNA insertion mutants. (From heterozygous GABI-362-D05 plants no homozygous progeny was obtained).

localized in exon 4 (SAIL-1288-E06 and SALK-151687) and one in exon 7 (SAIL-675-D09), respectively (Figure 5A). PCR analysis with T-DNA-specific and gene-specific primers revealed that all GABI and Syngenta mutants contain inverted T-DNA repeats. Positions of T-DNA insertions were confirmed by sequencing of PCR products from the corresponding genomic positions. Plants

heterozygous or homozygous for the T-DNA insertions were identified by PCR with pairs of gene-specific primers and gene-specific and T-DNA left border (LB)-specific primers. Homozygous mutants were identified for five insertion lines (GABI-068-A03, SALK-031919, SALK-151687, SAIL-1288E06 and SAIL-675D09). For the GABI-362-D05 mutant, PCR genotyping of progenies of

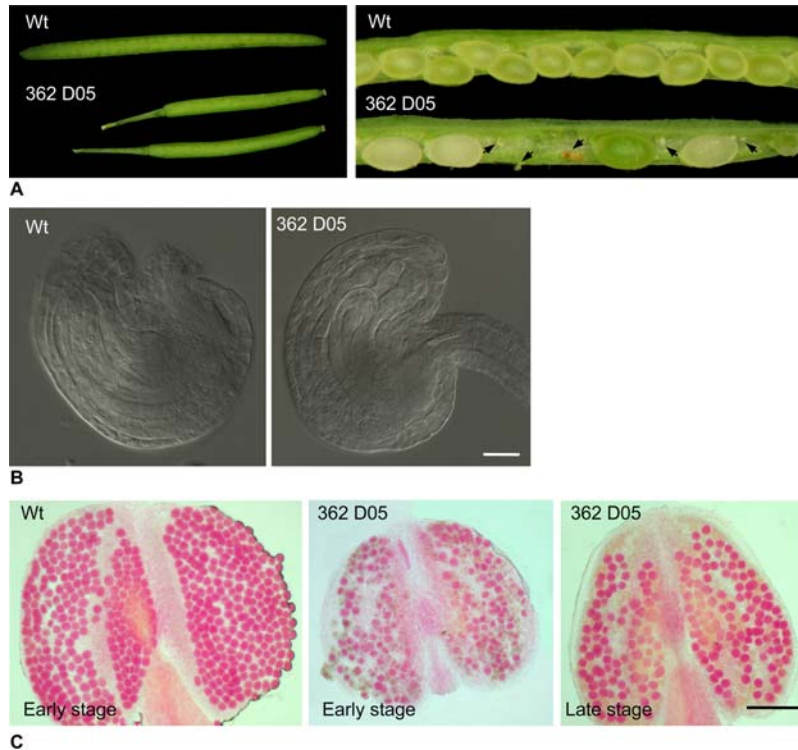


Figure 6. Seed development in the heterozygous *bub3.1* mutant GABI-362-D05. (A). Comparison of silique size from wild type and mutant plants (left). Open siliques from wild type and mutant (right). The mutant siliques contain normal seeds and undeveloped ovules. Ovules that remain unfertilized (arrowheads), and do not initiate seed development, degenerate and leave an empty space in the pod. (B) Wild type and one-nucleate mutant ovules. (C) Alexander staining of wild type and heterozygous *bub3.1* mutant anthers. Bars: (B) 20 μ m; (C) 100 μ m.

heterozygous individuals revealed no homozygous plants within three generations.

Semiquantitative RT-PCR was performed with all homozygous mutants to test for the presence of full length or truncated transcripts of *Bub3.1* and *Bub3.2* genes (Figure 5B). In case of the *bub3.1* GABI-068A03 mutant, no full length transcript was detected, however, a transcript starting downstream of the T-DNA insertion (P3+P2) was present. RT-PCR with the LB-specific and the P4 primer revealed that transcription started from T-DNA due to the presence of a 35S promoter within the T-DNA. Heterozygous GABI-362-D05 mutant plants displayed only a slight reduction of mRNA transcript level compared to wild type (data not shown). As expected, a full length transcript was detected in the SALK-031919 mutant. For all *bub3.2* mutants, no full length transcripts were detected (Figure 5B). Since Syngenta mutants do not contain a 35S promoter within the T-DNA (19), transcripts starting within the T-DNA insertion can be excluded for the SAIL-1288-E06 and SAIL-675-D09 mutants. Transcripts from upstream the T-DNA are most likely too short to encode a functional protein. In case of the SALK-151687 mutant, a transcript downstream the T-DNA insertion, possibly generated by 35S promoter present in T-DNA, was detected. Functional proteins encoded by short transcripts from upstream or downstream the T-DNA insertion of SALK-151687 are rather unlikely.

4.5. Characterization of embryo lethal *bub3.1* mutant (GABI-362D05)

Segregation analysis of GABI-362-D05 mutant seedlings on sulfadiazine containing medium revealed a 6:1 ratio of *sulf^r*:*sulf^s* progeny indicating the presence of an additional T-DNA insertion. To separate these insertions, GABI-362-D05 individuals were crossed to wild type. Seeds of the F2 of this cross were tested for sulfadiazine resistance. A 2:1 ratio of *sulf^r*:*sulf^s* progeny was obtained, what is typical for embryo lethal mutants with a single T-DNA insertion (29). Linkage of the insert to the sulfadiazine resistance gene was demonstrated by PCR with DNA isolated from 48 individuals and with pairs of *Bub3.1* gene-specific primers and with the gene-specific and the LB-GABI primer. All tested individuals appeared to be heterozygous for the T-DNA insertion within the *Bub3.1* gene and no homozygous plants were recovered.

The GABI-362-D05 mutant plants were morphologically similar to wild type plants under normal growth conditions and developed normal roots, leaves, shoots, and flowers. Since no homozygous plants were found, siliques were analyzed for seed abortion. Ten siliques from each of ten individual plants revealed about 66% of aborted seeds. As a result of the ovule abortion, heterozygous GABI-362-D05 mutant plants are semi-sterile and show a reduced silique length (Figure 6A).

Since Bub3.1 function might be important for female and for male gametophytes, we examined pollen viability and ovule development of the GABI-362-D05 mutant. On average, ten anthers were analyzed from each of 10 mutant plants and of two wild type plants. In flower buds of the same stage, pollen development of the mutant was delayed compared to the wild type. Then, pollen viability was tested in mutant flower buds of a later stage (Figure 6C). The mutant anthers were generally smaller than that of the wild type and contained less pollen grains.

Within the same flower bud, ovules and gametophytes develop synchronously (30, 31). Thus, cleared whole-mount ovules from a semi-sterile plant heterozygous for a megagametophytic mutation allow comparison of mutant and wild type embryo sacs within the same gynoecium. The analysis of ovule development in the heterozygous GABI-362-D05 mutant showed that some ovules were arrested at one-nucleate stage (before gametophytic mitoses), while other (wild type) ovules were already in multinucleate stage (Figure 6B).

5. DISCUSSION

In contrast to other organisms, *Arabidopsis* contains three instead of only one isoform of Bub3. The high similarity of *Bub3.1* and *Bub3.2* sequences at the nucleotide level and a similar intron/exon structure (Figure 5B), suggest a recent duplication event for their origin, while *Bub3.3* displays relatively low similarity with the other two isoforms and its origin is less obvious. Until now no Bub3 homologues were identified and characterized in plants. However, for Mad2, the only spindle checkpoint protein identified and characterized so far in plants, different localization patterns were described. Wheat Mad2 localized in nuclei and cytoplasm during interphase, faint MAD2 signals were occasionally detected at chromosomes during prometaphase, while intense MAD2 signals were observed at the centromeres after colchicine-mediated metaphase arrest (6). Maize Mad2 was found at kinetochores that were not attached to microtubules during prometaphase, or when the microtubules were depolymerised due to oryzalin exposure, but not during interphase (7).

The Bub3 protein is a good candidate to mediate assembly of protein complexes in response to kinetochore checkpoint activation because it contains WD40 motifs, known to be involved in protein-protein interactions (32). Indeed, point mutations altering the conserved WD40 motifs of yeast Bub3 disrupt its association with Mad2, Mad3 and Cdc20 and abolish correct checkpoint response. Therefore, Bub3 was proposed to serve as a platform for interactions between checkpoint proteins (33).

All three *Arabidopsis* Bub3 homologues contain WD40-repeats, Bub3.1 and Bub3.2 proteins have three WD40 repeats, while Bub3.3 has only two. In contrast, human Bub3 is a protein with four WD40 repeats (34). A different number of WD40 repeats in Bub3 proteins of different organisms possibly indicates a different composition of checkpoint complexes in the corresponding organisms.

Fusion proteins of Bub3 either with EYFP or with ECFP yielded fluorescence within nuclei of transformants independent of the expression level of the fusion protein. However, no fluorescence was detected on chromosomes. A nuclear localization of GFP-Bub3 and Bub3-GFP was also shown in human cell cultures and in yeast (34, 35), and also for the *Xenopus* egg extracts using anti-Bub3 antibodies (36). In contrast to *Arabidopsis*, human and *Xenopus* Bub3 proteins were localized at centromeres during prometaphase. However, in some other organisms spindle checkpoint proteins were clearly visible at centromeres only after application of microtubule depolymerizing inhibitors (6, 35). Due to the low amount of mitotic cells, treatment of *Arabidopsis* seedlings with such inhibitors is less effective than treatment of cell suspensions. Moreover, in *Arabidopsis*, endoreplication cycles, omitting G2 and mitosis, occur in addition to the mitotic cell cycle and generate endopolyploid nuclei (37, 38). Therefore, *Arabidopsis* might be rather resistant to treatment with microtubule depolymerizing agents that causes mitotic arrest. Germination of *Arabidopsis* wild type seeds on medium containing 10 μ M propyzamide resulted in an increased level of endopolyploidization (data not shown). Comparison of the proportions of 2C-64C nuclei in *Arabidopsis* seedlings germinated on control medium with those germinated on medium with 10 μ M propyzamide indicates that propyzamide treatment leads to inhibition of mitosis and concomitantly to initiation of endocycles. It is also possible that Bub3 is not detectable at *Arabidopsis* centromeres because of the small amount of molecules present at centromeres of the rather small chromosomes.

Knockout of *Bub3.1* and *Bub3.2* genes via the T-DNA insertions indicate different functional importance for both isoforms. Bub3.1 appeared to be essential during embryogenesis since a *bub3.1* null mutant is embryo-lethal and no homozygous plants were obtained, while three different *bub3.2* mutant alleles survived in homozygous state without severe disturbances of growth and development. Either Bub3.2 can be substituted by another protein, or Bub3.2 has not developed a specific function since its recent evolutionary appearance by gene duplication, but rather lost its functionality since Bub3.2 is not able to compensate for the loss of Bub3.1. Also inactivation of the mouse *Bub3* gene by interrupting its coding region showed an embryo lethal phenotype since no homozygous mutants were obtained, while Bub3^{+/-} mice were indistinguishable from wild type (39, 40).

In contrast, Bub3 of yeast seems not to be essential under normal growth conditions, because under these conditions homozygous *bub3* mutants are viable. However, yeast Bub3 was shown to be important for the response to spindle damage induced by microtubule depolymerizing inhibitors (3).

6. ACKNOWLEDGMENT

We thank Andrea Kunze for technical assistance, Karin Lipfert and Ursula Tiemann for help with preparation of figures, David Koszegi for help with ovules analysis. This work was supported by a grant from the Deutsche Forschungsgemeinschaft to I.S. (Schu 951/9-3).

7. REFERENCES

1. Nicklas R. B.: How cells get the right chromosomes. *Science* 275, 632-637 (1997)
2. Li R., A. W. Murray: Feedback control of mitosis in budding yeast. *Cell* 66, 519-531 (1991)
3. Hoyt M. A., L. Totis, B. T. Roberts: *S. cerevisiae* genes required for cell cycle arrest in response to loss of microtubule function. *Cell* 66, 507-517 (1991)
4. Musacchio A., K. G. Hardwick: The spindle checkpoint: structural insights into dynamic signalling. *Nat Rev Mol Cell Biol* 3, 731-741 (2002)
5. Yu H.: Regulation of APC-Cdc20 by the spindle checkpoint. *Curr Opin Cell Biol* 14, 706-714 (2002)
6. Kimbara J., T. R. Endo, S. Nasuda: Characterization of the genes encoding for MAD2 homologues in wheat. *Chromosome Res* 12, 703-714 (2004)
7. Yu H.-G., M. G. Muszynski, R. K. Dawe: The maize homologue of the cell cycle checkpoint protein MAD2 reveals kinetochore substructure and contrasting mitotic and meiotic localization patterns. *J Cell Biol* 145, 425-435 (1999)
8. Abrieu A., L. Magnaghi-Jaulin, J. A. Kahana, M. Peter, A. Castro, S. Vigneron, T. Lorca, D. W. Cleveland, J. C. Labbé: Mps1 is a kinetochore-associated kinase essential for the vertebrate mitotic checkpoint. *Cell* 106, 83-93 (2001)
9. Dobles M., V. Liberal, M. L. Scott, R. Benezra, P. K. Sorger: Chromosome missegregation and apoptosis in mice lacking the mitotic checkpoint protein Mad2. *Cell* 101, 635-645 (2000)
10. Taylor S. S., D. Hussein, Y. Wang, S. Elderkin, C. J. Morrow: Kinetochore localisation and phosphorylation of the mitotic checkpoint components Bub1 and BubR1 are differentially regulated by spindle events in human cells. *J Cell Sci* 114, 4385-4395 (2001)
11. Rieder C. L., R. W. Cole, A. Khodjakov, G. Sluder: The checkpoint delaying anaphase in response to chromosome monoorientation is mediated by an inhibitory signal produced by unattached kinetochores. *J Cell Biol* 130, 941-948 (1995)
12. Howell B. J., B. Moree, E. M. Farrar, S. Stewart, G. Fang, E. D. Salmon: Spindle checkpoint protein dynamics at kinetochores in living cells. *Curr Biol* 14, 953-964 (2004)
13. Fang G.: Checkpoint protein BubR1 acts synergistically with Mad2 to inhibit anaphase-promoting complex. *Mol Biol Cell* 13, 755-766 (2002)
14. Sudakin V., G. K. T. Chan, T. J. Yen: Checkpoint inhibition of the APC/C in HeLa cells is mediated by a complex of BUBR1, BUB3, CDC20, and MAD2. *J Cell Biol* 154, 925-936 (2001)
15. Tang Z., R. Bharadwaj, B. Li, H. Yu: Mad2-Independent inhibition of APC^{Cdc20} by the mitotic checkpoint protein BubR1. *Dev Cell* 1, 227-237 (2001)
16. Roberts B. T., K. A. Farr, M. A. Hoyt: The *Saccharomyces cerevisiae* checkpoint gene *BUB1* encodes a novel protein kinase. *Mol Cell Biol* 14, 8282-8291 (1994)
17. Bernard P., K. Hardwick, J.-P. Javerzat: Fission yeast Bub1 is a mitotic centromere protein essential for the spindle checkpoint and the preservation of correct ploidy through mitosis. *J Cell Biol* 143, 1775-1787 (1998)
18. Basu J., H. Bousbaa, E. Logarinho, Z. Li, B. C. Williams, C. Lopes, C. E. Sunkel, M. L. Goldberg: Mutations in the essential spindle checkpoint gene *bub1* cause chromosome missegregation and fail to block apoptosis in *Drosophila*. *J Cell Biol* 146, 13-28 (1999)
19. Sessions A., E. Burke, G. Presting, G. Aux, J. McElver, D. Patton, B. Dietrich, P. Ho, J. Bacwaden, C. Ko, J. D. Clarke, D. Cotton, D. Bullis, J. Snell, T. Miguel, D. Hutchison, B. Kimmerly, T. Mitzel, F. Katagiri, J. Glazebrook, M. Law, S. A. Goff: A high-throughput *Arabidopsis* reverse genetics system. *Plant Cell* 14, 2985-2994 (2002)
20. Rosso M. G., Y. Li, N. Strizhov, B. Reiss, K. Dekker, B. Weisshaar: An *Arabidopsis thaliana* T-DNA mutagenized population (GABI-Kat) for flanking sequence tag-based reverse genetics. *Plant Mol Biol* 53, 247-259 (2003)
21. Lermontova I., V. Schubert, J. Fuchs, S. Klatte, J. Macas, I. Schubert: Loading of *Arabidopsis* centromeric histone CENH3 occurs mainly during G2 and requires the presence of the histone fold domain. *Plant Cell* 18, 2443-2451 (2006)
22. Alexander M. P.: Differential staining of aborted and nonaborted pollen. *Stain Technol* 44, 117-122 (1969)
23. Bradford M. M.: A rapid and sensitive method for the quantitation of microgram quantities of protein utilizing the principle of protein-dye binding. *Anal Biochem* 72, 248-254 (1976)
24. Laemmli U. K.: Cleavage of structural proteins during the assembly of the head of bacteriophage T4. *Nature* 227, 680-685 (1970)
25. Neer E. J., C. J. Schmidt, R. Nambudripad, T. F. Smith: The ancient regulatory-protein family of WD-repeat proteins. *Nature* 371, 297-300 (1994)
26. Menges M., J. A. H. Murray: Synchronous *Arabidopsis* suspension cultures for analysis of cell-cycle gene activity. *Plant J* 30, 203-212 (2002)
27. Ito M., M. Iwase, H. Kodama, P. Lavis, A. Komamine, R. Nishihama, Y. Machida, A. Watanabe: A novel *cis*-acting element in promoters of plant B-type cyclin genes activates M phase-specific transcription. *Plant Cell* 10, 331-341 (1998)
28. Shaul O., V. Mironov, S. Burssens, M. Van Montagu, D. Inzé: Two *Arabidopsis* cyclin promoters mediate distinctive transcriptional oscillation in synchronized tobacco BY-2 cells. *Proc Natl Acad Sci USA* 93, 4868-4872 (1996)
29. Errampalli D., D. Patton, L. Castle, L. Mickelson, K. Hansen, J. Schnall, K. Feldmann, D. Meinke: Embryonic lethals and T-DNA insertional mutagenesis in *Arabidopsis*. *Plant Cell* 3, 149-157 (1991)
30. Christensen C., E. J. King, J. R. Jordan, G. N. Drews: Megagametogenesis in *Arabidopsis* wild type and the Gf mutant. *Sexual Plant Reproduction* 10, 49-64 (1997)
31. Schneitz K., M. Hülskamp, R. E. Pruitt: Wild-type ovule development in *Arabidopsis thaliana*: a light microscope study of cleared whole-mount ovules. *Plant J* 7, 731-749 (1995)
32. Smith T. F., C. Gaitatzes, K. Saxena, E. J. Neer: The WD repeat: a common architecture for diverse functions. *Trends Biochem Sci* 24, 181-185 (1999)
33. Fraschini R., A. Beretta, L. Sironi, A. Musacchio, G. Lucchini, S. Piatti: Bub3 interaction with Mad2, Mad3 and Cdc20 is mediated by WD40 repeats and does not require intact kinetochores. *Embo J* 20, 6648-6659 (2001)
34. Taylor S. S., E. Ha, F. McKeon: The human homologue of Bub3 is required for kinetochore localization

of Bub1 and a Mad3/Bub1-related protein kinase. *J Cell Biol* 142, 1-11 (1998)

35. Kerscher O., L. B. Crotti, M. A. Basrai: Recognizing chromosomes in trouble: association of the spindle checkpoint protein Bub3p with altered kinetochores and a unique defective centromere. *Mol Cell Biol* 23, 6406-6418 (2003)

36. Campbell L., K. G. Hardwick: Analysis of Bub3 spindle checkpoint function in *Xenopus* egg extracts. *J Cell Sci* 116, 617-628 (2003)

37. Brodsky W. Y., I. V. Uryvaeva: Cell polyploidy: its relation to tissue growth and function. *Int Rev Cytol* 50, 275-332 (1977)

38. D'Amato F.: Chromosome endoreduplication in plant tissue development and function. In: Plant cell proliferation and its regulation in growth and development. Eds: Bryant J. A., Chiatante D. John Wiley & Sons, Chichester (1998)

39. Babu J. R., K. B. Jeganathan, D. J. Baker, X. Wu, N. Kang-Decker, J. M. van Deursen: Rael is an essential mitotic checkpoint regulator that cooperates with Bub3 to prevent chromosome missegregation. *J Cell Biol* 160, 341-353 (2003)

40. Kalitsis P., E. Earle, K. J. Fowler, K. H. A. Choo: *Bub3* gene disruption in mice reveals essential mitotic spindle checkpoint function during early embryogenesis. *Genes Dev* 14, 2277-2282 (2000)

Key Words: *Arabidopsis*, Bub3, Mitosis, Spindle Checkpoint

Send correspondence to: Dr. Inna Lermontova, Leibniz-Institute of Plant Genetics and Crop Plant Research (IPK), D-06466 Gatersleben, Germany, Tel: 49-39482-5537, Fax: 49-39482-5137, E-mail: lermonto@ipk-gatersleben.de

<http://www.bioscience.org/current/vol13.htm>